

Minimax properties of conditional entropy and quantum discord for XXZ symmetric quantum states

M. A. Yurischev*

Institute of Problems of Chemical Physics of the Russian Academy of Sciences, 142432 Chernogolovka, Moscow Region, Russia

Abstract

We consider the XXZ subclass of symmetric two-qubit X states and study for it the behavior of quantum conditional entropy S_{cond} as a function of measurement angle $\theta \in [0, \pi/2]$. Numerical calculations show that the function $S_{cond}(\theta)$ for X states can have at most a one local extremum in the open interval $(0, \pi/2)$. If the extremum is a minimum the quantum discord displays regions with variable (state dependent) optimal measurement angle θ^* . Such θ -regions (phases, fractions) are very tiny in the space of X states. We also discover the cases when the conditional entropy has a local *maximum* inside the interval $(0, \pi/2)$. It is remarkable that the maximum exist in surprisingly wide regions and the boundaries for such regions are determined by the same bifurcation conditions as for those with a minimum.

1 Introduction

Quantum correlations lie at the heart of quantum information science. Different measures have been proposed to quantify them. Owing to the crucial role in a number of quantum information problems and particularly in the algorithm of deterministic quantum computation with one pure qubit (DQC1), special place among those measures belongs to the quantum discord [1, 2, 3, 4].

The notion of information-theoretic quantum discord, Q , for a bipartite system, AB , has been introduced by Zurek in 2000 [5]. He defined the quantum discord as a difference between the quantum generalizations of symmetric and asymmetric forms of classical mutual information. This difference depends on the measurement which is performed on a subsystem (say, B) to obtain the quantum conditional entropy S_{cond} entering in the asymmetric form of quantum mutual information. As a result, the definition of quantum discord was reduced to the relation $Q = S(\rho_B) - S(\rho_{AB}) + S_{cond}$, where $S(\rho_{AB})$ and $S(\rho_B)$ are the entropies for the quantum states ρ_{AB} and ρ_B of joint system AB and its subsystem B , respectively. To eliminate the undesirable dependence of quantum discord on the specific measurement, one performs optimization over all measurements. It may be a minimization or, v.v., maximization. Taking into account physical (information-theoretic) reasoning, the minimization over the complete set of local orthogonal-projective (von Neumann) measurements $\{\Pi_i\}$ has been

*E-mail: yur@itp.ac.ru

taken in the final definition of quantum discord [6, 7]. Another possible invariant quantity, namely the maximized discord, remained outside the attention.

Notice, the orthogonal projectors $\{\Pi_i = |i'\rangle\langle i'|\}$ can be parametrized by two angles θ , ϕ : $|0'\rangle = \cos(\theta/2)|0\rangle + e^{i\phi}\sin(\theta/2)|1\rangle$ and $|1'\rangle = e^{-i\phi}\sin(\theta/2)|0\rangle - \cos(\theta/2)|1\rangle$. Thus, the optimization for the general two-qubit systems is reduced to that over two variables.

Due to the optimization procedure, evaluation of quantum discord in practice entails great difficulties even for the two-qubit systems. Closed analytical formula up to the present has been derived only for the Bell-diagonal states [8].

An attempt to extend the success of Luo [8] to the X states was undertaken in 2010 by Ali, Rau, and Alber [9]. Unfortunately, the authors decided that the extreme values of parameters which characterize the von Neumann measurement are attained only at their end points. Shortly after, however, the counterexamples of X density matrices have been given which demonstrate a conditional entropy minimum inside the measurement parameter interval [10, 11]. Thus, the analytic formula of Ref. [9] is incorrect in general.

At that time it was also established that for X states the optimization of conditional entropy (and hence discord) over the projectors $\{\Pi_i(\theta, \phi)\}$ can be worked out exactly over the azimuthal angle ϕ but one optimization procedure, in the polar angle $\theta \in [0, \pi/2]$, remains relevant [12, 13, 14]. As a result, a pessimistic verdict has been made: “For general two-qubit X states quantum discord cannot be evaluated analytically” [15] (see also [16] and [17]¹).

Definite optimism was restored in Refs. [18, 19, 20], where it has been observed that the formula for calculating the quantum discord of two-qubit X states has, in any event, a semianalytical or actually almost analytical form

$$Q = \min\{Q_0, Q_{\theta^*}, Q_{\pi/2}\}. \quad (1)$$

Here the branches Q_0 and $Q_{\pi/2}$ are the analytical expressions (corresponding to the discord with optimal measurement angles 0 and $\pi/2$, respectively) and only the third branch Q_{θ^*} requires one-dimensional searching the local optimal measurement angles $\theta^* \in (0, \pi/2)$. Notice, a similar situation with the variable optimal angle can also occur for the one way-quantum deficit of two-qubit X states [21].

Three possible regions Q_0 , $Q_{\pi/2}$, and Q_{θ^*} are separated between themselves in the density-matrix parameter space by the sharp demarcation boundaries. An equation for the boundary between Q_0 and $Q_{\pi/2}$ regions (phases) is, obviously, $Q_0 = Q_{\pi/2}$ or $S_{cond}(0) = S_{cond}(\pi/2)$. The equations for 0- and $\pi/2$ -boundaries separated respectively Q_0 and $Q_{\pi/2}$ regions with Q_{θ^*} one have the forms [18, 19, 20]

$$S''_{cond}(0) = 0, \quad S''_{cond}(\pi/2) = 0, \quad (2)$$

where $S''_{cond}(0)$ and $S''_{cond}(\pi/2)$ are the second derivatives of function $S_{cond}(\theta)$ with respect to θ at the end points $\theta = 0$ and $\pi/2$.

Equations (2) are based on the idea of bifurcation mechanism [22] for appearance and disappearance of intermediate local extremum: by varying the parameters of density matrix elements the inner extremum of $S_{cond}(\theta)$ can come into the interval $(0, \pi/2)$ or come out from it only through the end points $\theta = 0, \pi/2$. Bifurcation mechanism is supported by following two properties of function $S_{cond}(\theta)$. On the one hand, its first derivatives at $\theta = 0$ and $\pi/2$ identically equal zero, $S'_{cond}(0) \equiv S'_{cond}(\pi/2) \equiv 0$. This follows from direct calculations for

¹ Unfortunately, the authors of Ref. [17] have made a few mistakes. In particular, their equation (23) is incorrect and their conclusion about existence of the region with mysterious measurement $\sigma_?$ is wrong.

the function $S_{cond}(\theta)$ which is known in general X-state case ([20] and references therein). On the other hand, we suppose the unimodal property for the function $S_{cond}(\theta)$ (see Appendix). So, if the unimodality hypothesis is valid then the only possibility (except the trivial case $S_{cond}(\theta) = const$) to appear or disappear a single local extremum (minimum or maximum) inside the open interval by continue varying the parameters defining the X state is a doubling the extremum at the ends of interval $[0, \pi/2]$. Such a bifurcation mechanism for sudden birth (creation) and sudden death (annihilation) of interior extremum has been proposed by the author in Refs. [18, 19, 20]. Ones both equations (2) have been solved and it was found that the boundaries do not coincide between themselves, one should check the shape of curve $S_{cond}(\theta)$ inside the found corridor. If the curve exhibits the inner local extremum hence this will prove that the region under question exists in fact. Moreover, by this we can distinguish either the region contains the minimum or maximum.

The remainder of this article is arranged as follows. Domain of discord function is given in Sec. 2, complete three-dimensional discord phase diagram is presented in Sec. 3, regions with the intermediate minimum and maximum of conditional entropy are found, respectively, in Secs. 4 and 5. The results obtained are briefly summarized in Sec. 6. Finally, the Appendix includes material concerning the unimodal functions.

2 Density matrix and domain of definition for its entries

Density matrix ρ_{AB} of general two-qubit X state contains seven independent parameters. However, it is well known (see, e.g, [18]) such a density matrix can be reduced by using local unitary transformations to the real five-parameter form

$$\rho_{AB} = \frac{1}{4}(1 + s_1\sigma_z \otimes 1 + s_21 \otimes \sigma_z + c_1\sigma_x \otimes \sigma_x + c_2\sigma_y \otimes \sigma_y + c_3\sigma_z \otimes \sigma_z), \quad (3)$$

where σ_α ($\alpha = x, y, z$) are the Pauli matrices. The coefficients s_1, s_2, c_1, c_2, c_3 are the unary and binary correlation functions, i.e., experimentally measurable quantities. It is clear that

$$-1 \leq s_1, s_2, c_1, c_2, c_3 \leq 1. \quad (4)$$

The domain of definition, \mathcal{D} , in the five-dimensional space spanned by $(s_1, s_2, c_1, c_2, c_3)$ is formed according to the requirement of density-matrix positive semidefiniteness which leads to the conditions [11, 20, 23] (see also [24])

$$(1 - c_3)^2 \geq (s_1 - s_2)^2 + (c_1 + c_2)^2, \quad (1 + c_3)^2 \geq (s_1 + s_2)^2 + (c_1 - c_2)^2. \quad (5)$$

The solid \mathcal{D} is finite, lies in the five-dimensional hypercube $[-1, 1]^5$ in conforming with Eq. (4), results from an intersection of two conic hypercylinders [20] in accord with Eq. (5), and its volume is about 8% of the hypercube one.

Having taken 10 000 randomly chosen two-qubit X states the authors [14] found that $\approx 99.8\%$ of such states belong to the phases Q_0 and $Q_{\pi/2}$. On the other hand, specific examples show that there are Q_{θ^*} -regions with sizes of order 10^{-4} and less (see below Sec. 4 and Fig. 7). Therefore, to inspect the five-dimensional domain \mathcal{D} with such a resolution, the running a fivefold nested loop on hypothetical 10 GHz processor² will require the time more than a thousand years!

² At present, the maximum clock frequency of Intel and AMD microprocessors is around 8.7-8.8 GHz.

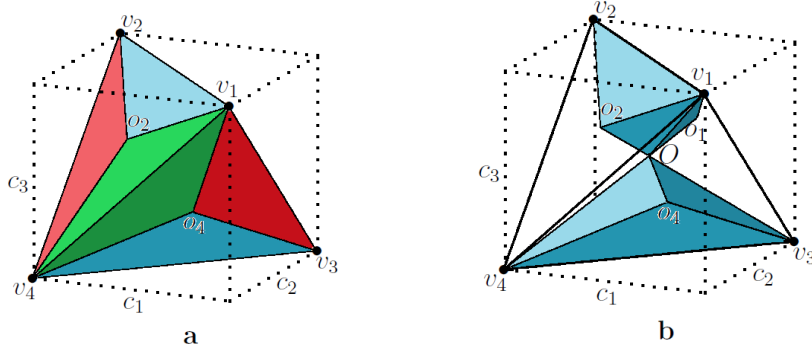


Figure 1: (Color online) Phase diagram for the discord function of Bell-diagonal states. The red, green, and blue regions are the domains of definition respectively for the three branches Q_1 , Q_2 , and Q_3 of discord function. Here, (a) is an outward appearance of tetrahedron $v_1v_2v_3v_4$ and (b) shows the Q_3 region; regions Q_1 and Q_2 are similar but include the pairs of edges $\{v_1v_3, v_2v_4\}$ and $\{v_1v_4, v_2v_3\}$, correspondingly

To avoid the arisen difficulty one can build up an atlas (collection) of "maps". In other words, it is reasonable to study different particular families of total X-state family. Here, we take an important in practice subclass of X states and perform for it careful investigation. But before, let us consider one classical example to extract useful inferences from it.

2.1 Luo's formula as an instructive example

A particular case $s_1 = s_2 = 0$ (i.e., when both local Bloch vectors are zero) corresponds to the Bell-diagonal states

$$\rho_{AB} = \frac{1}{4}(I + c_1\sigma_x \otimes \sigma_x + c_2\sigma_y \otimes \sigma_y + c_3\sigma_z \otimes \sigma_z). \quad (6)$$

Eigenvalues of this density matrix equal $p_1 = (1 + c_1 - c_2 + c_3)/4$, $p_2 = (1 - c_1 + c_2 + c_3)/4$, $p_3 = (1 + c_1 + c_2 - c_3)/4$, and $p_4 = (1 - c_1 - c_2 - c_3)/4$. Due to the nonnegativity definition of density operators, all $p_i \geq 0$ and therefore physical values of parameters c_1 , c_2 , and c_3 lie in the perfect tetrahedron which is inscribed in the three-dimensional cube $[-1, 1]^3$ and has the vertices $v_1 = (1, -1, 1)$, $v_2 = (-1, 1, 1)$, $v_3 = (1, 1, -1)$, and $v_4 = (-1, -1, -1)$ [25]; see Fig. 1. Faces of this tetrahedron are equilateral triangles and their centers are $o_1 = (1/3, 1/3, 1/3)$, $o_2 = (-1/3, -1/3, 1/3)$, $o_3 = (-1/3, 1/3, -1/3)$, and $o_4 = (1/3, -1/3, -1/3)$. Volume of this body equals a third of the $[-1, 1]^3$ cube volume.

The quantum discord of Bell-diagonal states is given by Luo's formula [8], which can be written as

$$Q = \min\{Q_1, Q_2, Q_3\}, \quad (7)$$

where

$$Q_i = \sum_{k=1}^4 p_k \log_2(4p_k) - \frac{1}{2}[(1 - c_i) \log_2(1 - c_i) + (1 + c_i) \log_2(1 + c_i)] \quad (8)$$

for $i = 1, 2, 3$. Luo's formula is perfect and has the same strong proof as, for example, Pythagoras' theorem.

Three possible cases $|c_1| \geq \max\{|c_2|, |c_3|\}$, $|c_2| \geq \max\{|c_1|, |c_3|\}$, and $|c_3| \geq \max\{|c_1|, |c_2|\}$ lead, as shown in Fig. 1, to a separation of tetrahedron by diagonal planes $|c_1| = |c_2|$, $|c_2| = |c_3|$, and $|c_3| = |c_1|$ respectively into three domains Q_1 , Q_2 , and Q_3 [20, 26]. Discord reaches maximal values (equal one in bit units) at the tetrahedron vertices and vanishes on the Cartesian axes Oc_1 , Oc_2 , and Oc_3 .

Call attention to that the quantum discord (7) is a piecewise-defined function. Because of this, when the system moves from one domain to another, the discord at the boundary experiences a sudden change which can be displayed as a fracture on its curve (see, e.g., a recent review [27]). This is similar to the first-order phase transitions which occur in liquids or solids.

In the case of Bell-diagonal states, the 0- and $\pi/2$ -boundaries coincide between themselves because both equations (2) are reduced to one relation $2|c_3| = |c_1 + c_2| + |c_1 - c_2|$, that is equivalent to four equations $c_3 = \pm c_1$ and $c_3 = \pm c_2$ (see Ref. [20]). These planes divide the tetrahedron into subdomains Q_0 and $Q_{\pi/2}$. The Q_0 -subdomain consists of two hexahedrons (O, v_1, v_2, o_1, o_2) and (O, v_3, v_4, o_3, o_4) ; they are shown in Fig. 1(b). Remaining volume of the tetrahedron belongs to the $Q_{\pi/2}$ states. It is larger in two times than the volume of Q_0 region.

Because the 0- and $\pi/2$ -boundaries are coincident between themselves, Q_{θ^*} -subdomain is absent and quantum discord is given by an explicit analytical formula $Q = \min\{Q_0, Q_{\pi/2}\}$ which is in full agreement with Eqs. (7) and (8). This becomes obvious if we take into account that the branch $Q_{\pi/2}(c_1, c_2, c_3)$ contains the piecewise functions like $|x|$ and therefore splits, in turn, into two subbranches, $Q_{\pi/2}^{(x)}$ and $Q_{\pi/2}^{(y)}$. As a result, the formula takes the form (see [20])

$$Q = \min\{Q_{\pi/2}^{(x)}, Q_{\pi/2}^{(y)}, Q_0\}, \quad (9)$$

where the branches $Q_{\pi/2}^{(x)}$, $Q_{\pi/2}^{(y)}$, and Q_0 correspond, respectively, to Q_1 , Q_2 , and Q_3 phases.

So, we learn useful lessons from the Bell-diagonal case and Luo's formula: the discord function is a piecewise one (this results, obviously, from the optimization condition) and the piecewise structure may be nested.

2.2 Domain for the XXZ-model with parity symmetry

Let us consider a two-qubit system with the three-parameter X density matrix

$$\rho_{AB} = \frac{1}{4} \begin{pmatrix} 1 + 2s_1 + c_3 & 0 & 0 & 0 \\ 0 & 1 - c_3 & 2c_1 & 0 \\ 0 & 2c_1 & 1 - c_3 & 0 \\ 0 & 0 & 0 & 1 - 2s_1 + c_3 \end{pmatrix}, \quad (10)$$

or in the Bloch form

$$\rho_{AB} = \frac{1}{4} [1 + s_1(\sigma_z \otimes 1 + 1 \otimes \sigma_z) + c_1(\sigma_x \otimes \sigma_x + \sigma_y \otimes \sigma_y) + c_3\sigma_z \otimes \sigma_z]. \quad (11)$$

Thus, the general X state (3) is restricted here by conditions $c_2 = c_1$ and $s_2 = s_1$. Such a model encounters often in different physically important problems.

Eigenvalues of matrix (10) are equal to $\lambda_{1,2} = (1 \pm 2s_1 + c_3)/4$ and $\lambda_{3,4} = (1 \pm 2c_1 - c_3)/4$. From the requirement $\rho_{AB} \geq 0$, it follows that all $\lambda_j \geq 0$ ($j = 1, \dots, 4$). As a result, the domain of definition of the discord function $Q(s_1, c_1, c_3)$ is a tetrahedron \mathcal{T} which is defined as

$$c_3 \in [-1, 1], \quad s_1 \in [-(1 + c_3)/2, (1 + c_3)/2], \quad c_1 \in [-(1 - c_3)/2, (1 - c_3)/2]. \quad (12)$$

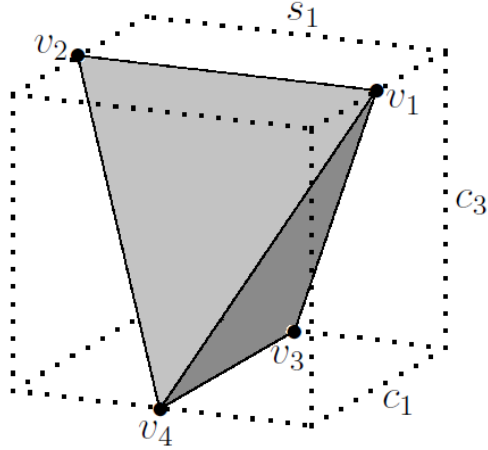


Figure 2: Shaded tetrahedron \mathcal{T} embedded in three-dimensional cube (dotted lines) is the domain of discord function $Q(s_1, c_1, c_3)$ for states (11)

This tetrahedron is enclosed in the three-dimensional cube $[-1, 1]^3$, has the vertices v_1, v_2, v_3 , and v_4 and isosceles triangle faces (see Fig. 2). Volume of tetrahedron \mathcal{T} equals a one sixth part of cube volume ($= 2^3$). So, one may say that the discord $Q(s_1, c_1, c_3)$ is a function on the tetrahedron \mathcal{T} .

It is easy to check that the matrices of structure (10) with different values of parameters, $\{s_1, c_1, c_3\}$ and $\{s'_1, c'_1, c'_3\}$, commute between themselves. Hence the fidelity, F , between two states ρ_{AB} and ρ'_{AB} can be calculated by simple formula

$$F = \left(\sum_{j=1}^4 \sqrt{\lambda_j \lambda'_j} \right)^2, \quad (13)$$

where λ'_j are the eigenvalues of matrix ρ'_{AB} with a form (10) but with parameters s'_1, c'_1 , and c'_3 . Fidelity is known to characterize a measure of closeness and distinguishability of quantum states.

The density matrix under discussion, Eqs. (10) or (11), can be map into the Gibbs density matrix ρ of the thermalized XXZ spin dimer in a homogeneous magnetic field applied in z -direction,

$$\rho = \frac{1}{Z} \exp(-H/T). \quad (14)$$

Here T is the temperature in energy units, Z is the partition function, and the Hamiltonian reads

$$H = -\frac{1}{2}[J(\sigma_x^1 \sigma_x^2 + \sigma_y^1 \sigma_y^2) + J_z \sigma_z^1 \sigma_z^2] - \frac{1}{2}B(\sigma_z^1 + \sigma_z^2), \quad (15)$$

where J and J_z are the exchange coupling constants and B is the external field. The energy levels of dimer equal

$$E_{1,2} = -\frac{1}{2}(J_z \pm 2B), \quad E_{3,4} = -\frac{1}{2}(J_z \pm 2J) \quad (16)$$

and therefore the partition function is given by

$$Z = 2 \left(e^{J_z/2T} \cosh \frac{B}{T} + e^{-J_z/2T} \cosh \frac{J}{T} \right). \quad (17)$$

Parameters of density matrix (11) equal

$$\begin{aligned} s_1 &= \frac{2}{Z} e^{J_z/2T} \sinh \frac{B}{T}, & c_1 &= \frac{2}{Z} e^{-J_z/2T} \sinh \frac{J}{T}, \\ c_3 &= \frac{2}{Z} \left(e^{J_z/2T} \cosh \frac{B}{T} - e^{-J_z/2T} \cosh \frac{J}{T} \right). \end{aligned} \quad (18)$$

Inversely, three parameters J , J_z , and B are expressed through the density matrix parameters s_1 , c_1 , c_3 and the temperature T as follows

$$J = \frac{T}{2} \ln \frac{1 + 2c_1 - c_3}{1 - 2c_1 - c_3}, \quad J_z = \frac{T}{2} \ln \frac{(1 + c_3)^2 - 4s_1^2}{(1 - c_3)^2 - 4c_1^2}, \quad B = \frac{T}{2} \ln \frac{1 + 2s_1 + c_3}{1 - 2s_1 + c_3}. \quad (19)$$

Thus, to gain an insight into the physical reasons we can translate different effects on a physical language of spin Hamiltonian as a function of temperature and magnetic field by different values of anisotropy parameter $\Delta = J_z/|J|$. The above relations allow to map $\{s_1, c_1, c_3\} \rightarrow \{T/|J|, B/|J|, \Delta\}$. Such a spin-model language is useful, e.g., in investigation of a spin detection efficiency of nonideal ferromagnetic detectors [28, 29, 30].

3 Branches Q_0 and $Q_{\pi/2}$. Phase diagram

The whole domain \mathcal{T} of discord function $Q(s_1, c_1, c_3)$ has been found in the previous section. Our next task is to determine the subdomains of \mathcal{T} which answer to different fractions of discord. We will solve this problem in two stages. As a preliminary, the tetrahedron \mathcal{T} will be divided into regions corresponding to the phases of pseudo-discord

$$\tilde{Q} = \min\{Q_0, Q_{\pi/2}\}. \quad (20)$$

Thereafter, in the next section, the phase Q_{θ^*} will be located in the solid \mathcal{T} .

Expressions for Q_0 and $Q_{\pi/2}$ as functions of matrix elements of the general X density matrix can be found in Refs. [15, 16, 18, 19, 20]³. Our case of interest is $s_2 = s_1$ and $c_2 = c_1$. In this particular case, quantum discord with the optimal measurement angle $\theta = 0$ is given by

$$\begin{aligned} Q_0(s_1, c_1, c_3) &= \frac{1}{4} [-2(1 - c_3) \ln(1 - c_3) \\ &+ (1 + 2c_1 - c_3) \ln(1 + 2c_1 - c_3) + (1 - 2c_1 - c_3) \ln(1 - 2c_1 - c_3)]. \end{aligned} \quad (21)$$

(Here, the discord is in nat measurement units; to transform the discord in bit units, one should divide it by $\ln 2$.) The function (21) does not depend on s_1 , it is even with respect to c_1 and equals zero by $c_1 = 0$ (i.e., in the classical limit).

For the branch $Q_{\pi/2}$, we have

$$\begin{aligned} Q_{\pi/2}(s_1, c_1, c_3) &= -\frac{1}{2} \left[(1 + s_1) \ln(1 + s_1) + (1 - s_1) \ln(1 - s_1) \right. \\ &+ \left(1 + \sqrt{s_1^2 + c_1^2} \right) \ln \left(1 + \sqrt{s_1^2 + c_1^2} \right) + \left(1 - \sqrt{s_1^2 + c_1^2} \right) \ln \left(1 - \sqrt{s_1^2 + c_1^2} \right) \left. \right] \\ &+ \frac{1}{4} [(1 + 2c_1 - c_3) \ln(1 + 2c_1 - c_3) + (1 - 2c_1 - c_3) \ln(1 - 2c_1 - c_3) \\ &+ (1 + 2s_1 + c_3) \ln(1 + 2s_1 + c_3) + (1 - 2s_1 + c_3) \ln(1 - 2s_1 + c_3)]. \end{aligned} \quad (22)$$

³ In Eq. (19) of Ref. [20] the common multiplier $\frac{1}{4}$ in the expression for $\Lambda_{1,2}$ should be replaced by $\frac{1}{2}$ (as in Refs. [18, 19])

This function is symmetric both on s_1 and c_1 and equals zero by $c_1 = 0$.

Let us break up the tetrahedron \mathcal{T} on the regions Q_0 and $Q_{\pi/2}$ temporarily ignoring a possible existence of region Q_{θ^*} . In this case, the boundaries between the regions Q_0 and $Q_{\pi/2}$ are defined by the condition $Q_0 = Q_{\pi/2}$ and, taken into account Eqs. (21) and (22), can be found from the transcendental equation

$$2[-(1 - c_3) \ln(1 - c_3) + (1 + s_1) \ln(1 + s_1) + (1 - s_1) \ln(1 - s_1) + (1 + \sqrt{s_1^2 + c_1^2}) \ln(1 + \sqrt{s_1^2 + c_1^2}) + (1 - \sqrt{s_1^2 + c_1^2}) \ln(1 - \sqrt{s_1^2 + c_1^2})] - (1 + 2s_1 + c_3) \ln(1 + 2s_1 + c_3) - (1 - 2s_1 + c_3) \ln(1 - 2s_1 + c_3) = 0. \quad (23)$$

If c_3 is fixed then the boundaries will be symmetric under mirror reflections $s_1 \rightarrow -s_1$ and $c_1 \rightarrow -c_1$.

We will now slice up the tetrahedron \mathcal{T} by planes with different fixed values of $c_3 \in [-1, 1]$. By this, two other parameters, s_1 and c_1 , may vary according to Eq. (12) in the limits which are depend only on c_3 . Let be $c_3 = -1$, then $s_1 = 0$ and therefore we are moving on the edge v_3v_4 (see Fig. 2). In this case, the equation (23) leads to the solutions $c_1 = \pm 1$. On the edge v_3v_4 , the values of Q_0 are less than those of $Q_{\pi/2} = \ln 2$ nat (i.e., one bit) and hence

$$Q = \frac{1}{2}[(1 + c_1) \ln(1 + c_1) + (1 - c_1) \ln(1 - c_1)]. \quad (24)$$

It will be shown in the next section that the fraction Q_{θ^*} is absent when $c_3 \leq 0$ and therefore this expression yields true values for the discord. Thus, the discord is one bit at the vertices v_3 and v_4 and varies according to Eq. (24) between them reaching zero at the middle of edge v_3v_4 , i.e., when $c_1 = 0$.

If c_3 somewhat increases then the cross section of tetrahedron \mathcal{T} takes a shape of stretched rectangle at the two ends of which the regions $Q_{\pi/2}$ are located and the remaining flat of rectangle belongs to the region Q_0 . Phase diagram of discord at $c_3 = -0.5$ is shown in Fig. 3(a). Two boundaries between the regions $Q_{\pi/2}$ and Q_0 are some arcs which cross the Oc_1 axis (i.e., when $s_1 = 0$) at the points $c_1 = \pm c_3$. Notice for a reference that in the case under discussion ($c_3 = -0.5$), the values of c_1 on the arcs at $s_1 = \pm 0.25$ equal $\pm 0.656\ 390\ 9127$ (see Fig. 3(a)).

By further increasing the height of tetrahedron section, two subregions $Q_{\pi/2}$ will move towards one to another and meet by $c_3 = 0$ at the point $s_1 = c_1 = 0$. This situation is fixed in Fig. 3(b). Here the cross section of tetrahedron \mathcal{T} is a square.

When c_3 reaches positive values, the cross section will be a rectangle stretched now in the s_1 -direction. As this takes place, two subregions $Q_{\pi/2}$ begin to intersect one another and an overlap between them is appeared. Remarkably that their common part will be occupied now by the phase Q_0 . This is depicted in Fig. 3(c) for $c_3 = 0.1$. Here, the arcs are intersected on the axis Os_1 at the points $s_1 = \pm 0.316\ 191\ 1555$.

With more increasing the values of c_3 , the new inner phase Q_0 will increase and by $c_3 = 1/3$ the arcs touch the horizontal sides of the rectangle. Thereafter the region $Q_{\pi/2}$ will consist of four $Q_{\pi/2}$ -subregions isolated in the cross section. This situation is shown in Fig. 3(d) by $c_3 = 0.34$. Here, the arc-like curves are intersected at $s_1 = \pm 0.583\ 024$, reach the vertical sides ($s_1 = \pm 0.67$) of the rectangle at $c_1 = \pm 0.227$, and horizontal ones at $s_1 = \pm 0.113\ 737$.

In the limit $c_3 \rightarrow 1$, the Q_0 -phase becomes again the only dominant on the edge v_1v_2 but here the discord tends to zero because c_1 vanishes.

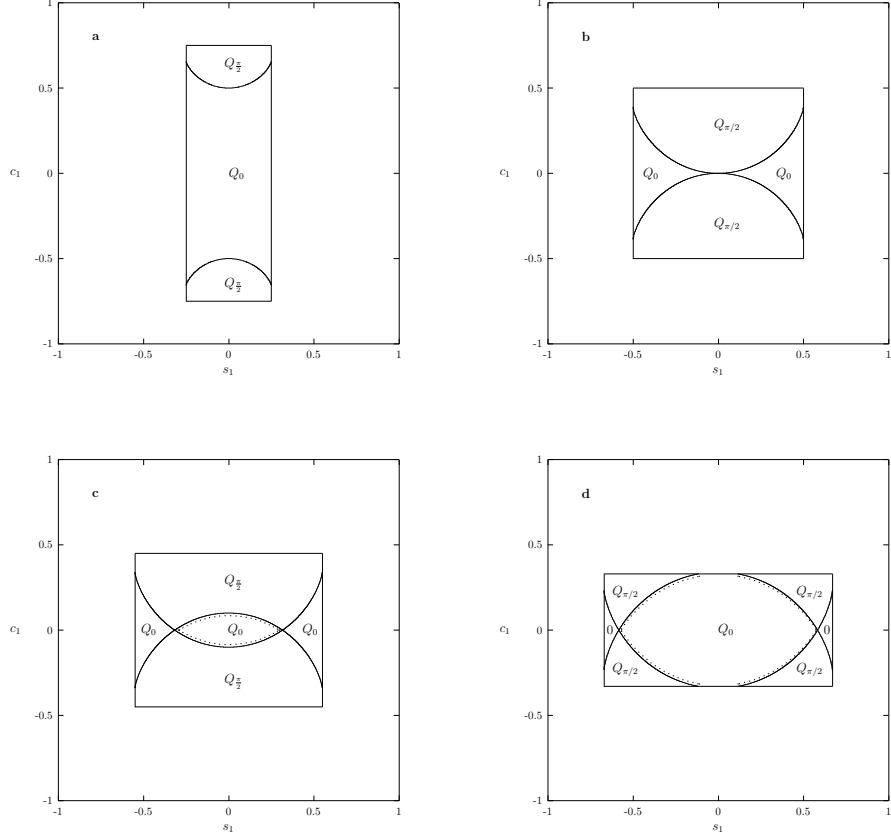


Figure 3: Phase diagrams for the discord by different sections of tetrahedron \mathcal{T} by planes $c_3 = -0.5$ (a), 0 (b), 0.1 (c), and 0.34 (d). (On the section (d), the region 0 is the same as Q_0 .) Boundaries between the phases Q_0 and $Q_{\pi/2}$ are shown by single solid lines. The Q_{θ^*} regions are thin too and cannot be resolved in the given scale; their positions are marked by double solid-dotted lines, see (c) and (d)

From the above analysis it is not difficult to reconstruct a three-dimensional picture — the solid $Q_{\pi/2}$ (or, v.v., Q_0) inside the tetrahedron \mathcal{T} . In the next sections, it will be shown that the phase diagrams presented in Fig. 3 are true for $c_3 \leq 0$ while when $c_3 > 0$ the inner region Q_0 and the $Q_{\pi/2}$ ones are separated between themselves by very thin layers which do not resolved in the scale of Fig. 3 and therefore their locations are shown schematically by the double solid-dotted lines.

4 Regions with the intermediate *minimum* of conditional entropy

To find the phase Q_{θ^*} we will study the behavior of conditional entropy shapes. Using again the general expression for the average quantum conditional entropy of five-parameter X state [18, 19, 20], we obtain that in case of interest $s_2 = s_1$ and $c_2 = c_1$ the entropy is given as

$$\begin{aligned}
& S_{cond}(\theta; s_1, c_1, c_3) \\
&= \ln 2 + \frac{1}{2}[(1 + s_1 \cos \theta) \ln(1 + s_1 \cos \theta) + (1 - s_1 \cos \theta) \ln(1 - s_1 \cos \theta)] \\
& - \frac{1}{4} \left[\left(1 + s_1 \cos \theta + \sqrt{(s_1 + c_3 \cos \theta)^2 + c_1^2 \sin^2 \theta} \right) \ln \left(1 + s_1 \cos \theta \right. \right. \\
& \quad \left. \left. + \sqrt{(s_1 + c_3 \cos \theta)^2 + c_1^2 \sin^2 \theta} \right) \right. \\
& + \left(1 + s_1 \cos \theta - \sqrt{(s_1 + c_3 \cos \theta)^2 + c_1^2 \sin^2 \theta} \right) \ln \left(1 + s_1 \cos \theta \right. \\
& \quad \left. - \sqrt{(s_1 + c_3 \cos \theta)^2 + c_1^2 \sin^2 \theta} \right) \\
& + \left(1 - s_1 \cos \theta + \sqrt{(s_1 - c_3 \cos \theta)^2 + c_1^2 \sin^2 \theta} \right) \ln \left(1 - s_1 \cos \theta \right. \\
& \quad \left. - \sqrt{(s_1 - c_3 \cos \theta)^2 + c_1^2 \sin^2 \theta} \right) \\
& + \left. \left(1 - s_1 \cos \theta - \sqrt{(s_1 - c_3 \cos \theta)^2 + c_1^2 \sin^2 \theta} \right) \ln \left(1 - s_1 \cos \theta \right. \right. \\
& \quad \left. \left. - \sqrt{(s_1 - c_3 \cos \theta)^2 + c_1^2 \sin^2 \theta} \right) \right]. \tag{25}
\end{aligned}$$

This function is differentiable at any point θ and, in full conformance with the statement made in the Introduction, its first derivatives with respect to θ identically equal zero for $\forall s_1, c_1, c_3 \in \mathcal{T}$ at the both ends of the interval $[0, \pi/2]$,

$$S'_{cond}(0; s_1, c_1, c_3) \equiv 0, \quad S'_{cond}(\pi/2; s_1, c_1, c_3) \equiv 0. \tag{26}$$

Let us investigate different types of conditional entropy behavior by various values of s_1 , c_1 , and c_3 belonging to the tetrahedron \mathcal{T} . For this purpose, we consider, for definiteness, a motion in the plane $c_3 = 0.34$ along the straight line $c_1 = 0.14$ when s_1 varies from zero to its maximal value $(1+c_3)/2 (= 0.67)$. This trajectory is shown by dotted horizontal line in Fig. 4. It intersects the boundaries defined by equation $Q_0 = Q_{\pi/2}$ at two points: $s_1^a = 0.473\,267$ and $s_1^b = 0.648\,435$ (see Fig. 4). When the values of s_1 are small enough, the curve of $S_{cond}(\theta)$ has monotonically increasing shape, i.e., its minimum lies at $\theta = 0$ and hence the quantum discord equals Q_0 . However, in the neighborhood of point s_1^a the curve is deformed and the intermediate minimum is arisen as depicted in Fig. 5(a)-(b). The largest depth of minimum is achieved near by $s_1 = s_1^a$ (see Fig. 5(c)). Here, $S_{cond}(0) = S_{cond}(\pi/2) = 0.816\,357\,3993$ bit and $S_{cond}^{min} = 0.816\,353\,3082$ bit which is achieved at $\theta = 0.732\,419 \approx 42^\circ$. Thus, the decrease is $\Delta S_{cond} = -0.000\,004\,09$ bit, i.e., relative decreasing equals 0.0005% only.

Thanks to the property (26) and because the minimum is single (what confirms the unimodality hypothesis/conjecture), the minimum could come into the open interval $(0, \pi/2)$ by continuous variation of state parameters only from the end point. Such a mechanism of bearing the inner minimum through a bifurcation (its doubling) is illustrated in Fig. 6 in wider window $-\pi \leq \theta \leq \pi$.

So, it is naturally to accept the unimodality hypothesis which allows to determine the sharp boundaries from Eqs. (2). Using Eq. (25) or general expressions from Refs. [18, 19, 20] we arrived at

$$S''_{cond}(0; s_1, c_1, c_3)$$

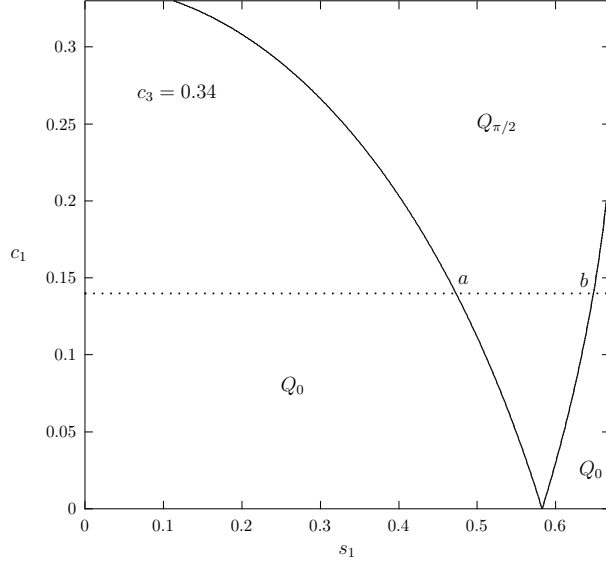


Figure 4: Quarter of a phase diagram by $c_3 = 0.34$. The dotted straight line $c_1 = 0.14$ crosses the $(Q_0-Q_{\pi/2})$ -boundaries at the points a and b in the vicinities of which the conditional entropy $S_{cond}(\theta)$ displays the intermediate minimum and maximum, respectively

$$\begin{aligned}
&= \frac{1}{4} \left[-c_1^2 \left(\frac{1}{s_1 + c_3} \ln \frac{1 + 2s_1 + c_3}{1 - c_3} + \frac{1}{s_1 - c_3} \ln \frac{1 - c_3}{1 - 2s_1 + c_3} \right) \right. \\
&\quad \left. s_1 \left(2 \ln \frac{1 - s_1}{1 + s_1} + \ln \frac{1 + 2s_1 + c_3}{1 - 2s_1 + c_3} \right) + c_3 \ln \frac{(1 + 2s_1 + c_3)(1 - 2s_1 + c_3)}{(1 - c_3)^2} \right] \quad (27)
\end{aligned}$$

and

$$\begin{aligned}
S''_{cond}(\pi/2; s_1, c_1, c_3) &= s_1^2 + \frac{c_1^2(s_1^2 + c_1^2 - c_3^2)}{2(s_1^2 + c_1^2)^{3/2}} \ln \frac{1 + \sqrt{s_1^2 + c_1^2}}{1 - \sqrt{s_1^2 + c_1^2}} \\
&\quad - \frac{s_1^2}{2} \left[\frac{1}{1 + \sqrt{s_1^2 + c_1^2}} \left(1 + \frac{c_3}{\sqrt{s_1^2 + c_1^2}} \right)^2 + \frac{1}{1 - \sqrt{s_1^2 + c_1^2}} \left(1 - \frac{c_3}{\sqrt{s_1^2 + c_1^2}} \right)^2 \right]. \quad (28)
\end{aligned}$$

Solving Eqs. (2) with these expressions we obtain the boundaries on the trajectory for the region Q_{θ^*} : it exists when $s_1 \in [0.473\,192\,8814, 0.473\,341\,2570]$. The width of given interval, 1.484×10^{-4} , is very small. Fidelity between the boundary states of found s_1 -interval is $F = 99.999\,998\%$, i.e., extremely high and therefore at present this Q_{θ^*} region cannot be detected experimentally.

In Fig. 7, the deviations $\Delta_0 = c_1^0 - c_1^\times$ and $\Delta_{\pi/2} = c_1^{\pi/2} - c_1^\times$ as functions of s_1 are drawn, where c_1^\times is the crossing point of the branches Q_0 and $Q_{\pi/2}$ (i.e., a solution of equation $Q_0 = Q_{\pi/2}$) and c_1^0 and $c_1^{\pi/2}$ are the 0- and $\pi/2$ -boundaries, i.e., the solutions of equations $S''_{cond}(0) = 0$ and $S''_{cond}(\pi/2) = 0$, respectively. Deviations vanish at $s_1 = 0.113\,737$ and $s_1 = 0.583\,024$; their maximum magnitudes lie at $s_1 = 0.471\,198$ and equal $\Delta_0^{max} = -0.000\,074\,1487$ and $\Delta_{\pi/2}^{max} = 0.000\,073\,7956$. Thus, the maximum width of Q_{θ^*} region in the c_1 -direction is 1.479×10^{-4} that is very tiny again.

It is interesting to understand what means the appearance and disappearance of intermediate region in the language of spin dimer at the thermal equilibrium; Eqs. (15)–(19).

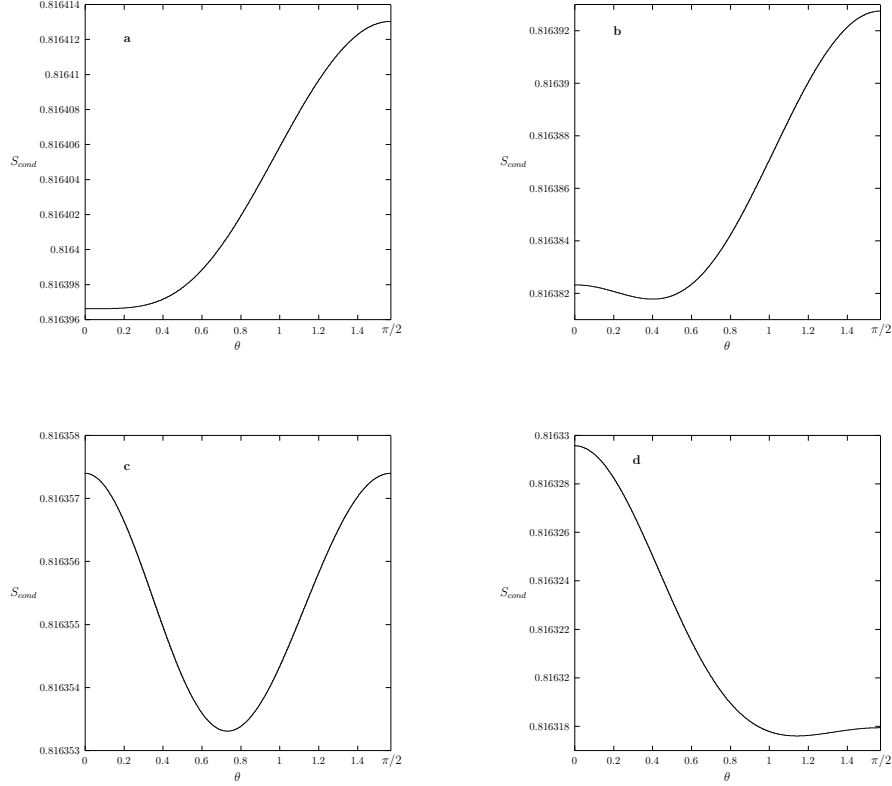


Figure 5: Conditional entropy S_{cond} (in bit units) vs measurement angle θ by $c_3 = 0.34$, $c_1 = 0.14$, and $s_1 = 0.473\ 193$ (a), $0.473\ 22$ (b), $0.473\ 267$ (c), $0.473\ 32$ (d). Here, the sudden birth, life, and sudden death of S_{cond} -minimum are observed

Taking $c_1 = 0.14$ and $c_3 = 0.34$ one gets $T/J = 2.111\ 082\ 372$ for any s_1 . When s_1 varies in the Q_{θ^*} region, that is from $s_1^0 = 0.473\ 192\ 8814$ to $s_1^{\pi/2} = 0.473\ 341\ 2570$, then the band for $\Delta = J_z/J$ lies between $1.019\ 558\ 9945$ and $1.020\ 248\ 4171$, i.e., the width of interval is now equal to $6.894\ 23 \times 10^{-4}$. At the same time, normalized magnetic field B/J varies from $1.942\ 519\ 04$ to $1.953\ 495\ 0495$. These results show that the phase Q_{θ^*} exists in a rather ordinary ferromagnetic region of dimer (both constants J and J_z are positive) and its sizes are very small as before.

On the other hand, taking $\Delta = 1.02$ (from the above found interval) and, for example, $B/J = 1$ the calculations yield that the conditional entropy has the intermediate minimum for T/J in the interval $[0.761\ 06, 0.853\ 61]$ which relative width equals 11.5% [18, 20]. So, the same Q_{θ^*} region can have large sizes on the phase diagram in (T, B) -variables by fixed Δ . This surprising result we interpret as follows. The phase Q_{θ^*} is a layer separating the Q_0 - and $Q_{\pi/2}$ -phases in the density matrix space (s_1, c_1, c_3) . This layer is thin in one direction only. Hence, if one considers the intermediate phase Q_{θ^*} in other directions the sizes may be large. However, even smallest fluctuations of system parameters (temperature, magnetic field, etc.) can lead away the phase Q_{θ^*} .

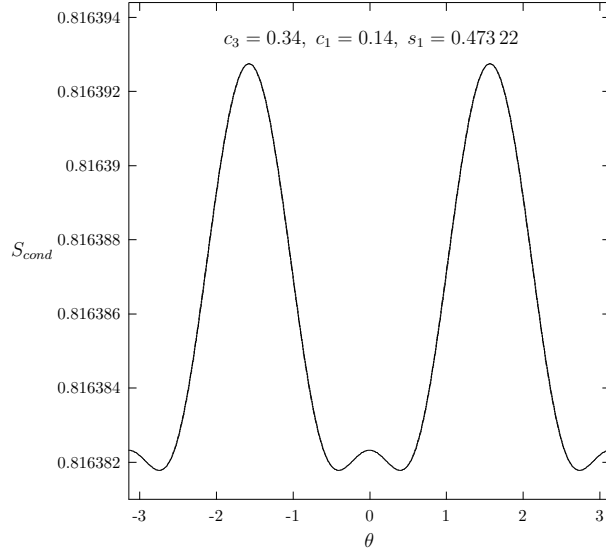


Figure 6: Conditional entropy S_{cond} (in bits) vs θ in the band $[-\pi, \pi]$ by $c_3 = 0.34$, $c_1 = 0.14$, and $s_1 = 0.47322$. This graph demonstrates the bifurcation of minimum at $\theta = 0$

5 Regions with the intermediate *maximum* of conditional entropy

We continue to go on the plane $c_3 = 0.34$ in the straightforward way $c_1 = 0.14$. In the interval where the phase Q_{θ^*} exists, the optimal measurement angle smoothly changes from zero to $\pi/2$ as can be seen from Fig. 5. Therefore, when $s_1 > 0.4733412570$, the discord equals $Q_{\pi/2}$ down to the neighborhood of point b (see Fig. 4). Near the point b a new phenomenon is observed. Namely, the extremum appears again but now instead of minimum a single maximum is arisen inside the interval $(0, \pi/2)$. This situation is shown in Fig. 8. The maximum as barrier separates two local minima at both bounds, $\theta = 0$ and $\pi/2$.

The maximum is born again thanks to the bifurcation mechanism but now the maximum at $\theta = 0$ splits into two maxima which are located upper and lower of this angle. To find the bounds where the maximum exists, we again solve the transcendental equations (2). Numerical calculations give the band $0.6477955876 \leq s_1 \leq 0.6491235832$. First, that catches the eye, is that the width of this interval, 1.37×10^{-3} , is considerably larger (in an order) than that for the minimum near the point a . Fidelity between the end states of the interval is here equal to $F = 99.99896\%$. This quantity is smaller in comparison with the fidelity for the region with minimum but it is again high too.

Largest excess of conditional entropy maximum is observed when $S_{cond}(0)$ equals $S_{cond}(\pi/2)$ (see Fig. 8(c)). This is achieved at $s_1 = 0.6484352971$ (i.e., with high accuracy at the middle of the interval with maximum). Here $S_{cond}(0) = S_{cond}(\pi/2) = 0.6538282081$ bit, $S_{cond}^{max} = 0.6539486436$ bit (it occurs at $\theta = 0.5994275584 \approx 34^\circ$) and the relative excess of the maximum equals 0.018% only.

Call attention that here, in contrast to the case with a minimum, the 0-boundary lies in the $Q_{\pi/2}$ region whereas the $\pi/2$ -boundary is in the Q_0 one. So, the boundaries go over one another and this cannot be realized in practice. Therefore, the only possibility for the discord is to change suddenly the optimal measurement angle (i.e., to jump from $\pi/2$ to 0)

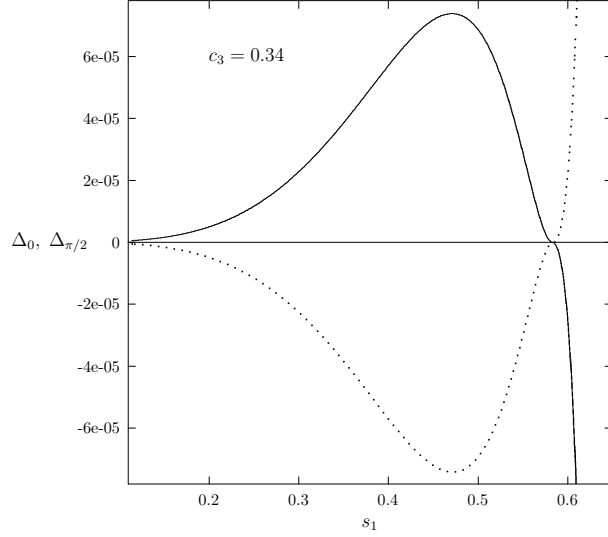


Figure 7: Deviations Δ_0 (dotted line) and $\Delta_{\pi/2}$ (solid line) vs s_1 in the cross section $c_3 = 0.34$

at the crossing point where $Q_{\pi/2} = Q_0$. Above this point the discord is again returned to the old value $Q_0 = 0.044\,231\,4345$ bit.

Evolution of quantum discord is shown in Fig. 9(1) from $s_1 = 0$ to 0.67 along the strait line $c_1 = 0.14$ in the section $c_3 = 0.34$. The curve has a minimum at the point with coordinates $(0.585, 0.027\,97)$. According to Eqs. (19), the coupling constant J_z changes its sign at $s_1 = 0.5997$ what correlates, more or less, with the above location of minimum on the curve Q upon s_1 .

Figure 9(2) shows the behavior of quantum discord in the vicinity of point a . It is clear seen how the Q_{θ^*} branch smoothly connect the branches Q_0 and $Q_{\pi/2}$. However, in spite of continuity and smoothness, the quantum discord Q experiences the sudden changes at both points $s_1^0 = 0.473\,192\,8814$ and $s_1^{\pi/2} = 0.473\,341\,2570$; non-analyticities are displayed in higher derivatives. This is in contrary to a statement of the authors [31] for POVM-measurements.

We carefully inspected the behavior of conditional entropy in different domains of tetrahedron \mathcal{T} . Our conclusions are follows. Regions with the intermediate maximum exist near all boundaries separating between themselves the phases Q_0 and $Q_{\pi/2}$ for both $c_3 < 0$ and $c_3 \geq 0$. These boundaries are shown in Fig. 3 by solid lines. Regions with the intermediate minimum of conditional entropy are available only by $c_3 > 0$ and exist as thin layers between the inner Q_0 region and $Q_{\pi/2}$ ones. Their locations are schematically shown in Fig. 3 by double solid-dotted lines and their structure is illustrated in Fig. 7. One can say that here a “sandwich”-like structure takes place. Volume of the three-dimensional Q_{θ^*} layer gives an estimation of corresponding states in the tetrahedron \mathcal{T} .

6 Conclusions

In the present paper, the discord phase diagram of X states with $s_1 = s_2$ and $c_1 = c_2$ has been built up. Location and exact boundaries for the discordant θ -fraction have been established.

We have also found the different types of conditional entropy behavior by various values of parameters s_1 , c_1 , and c_3 belonging to their full domain of definition \mathcal{T} . Firstly, the curve

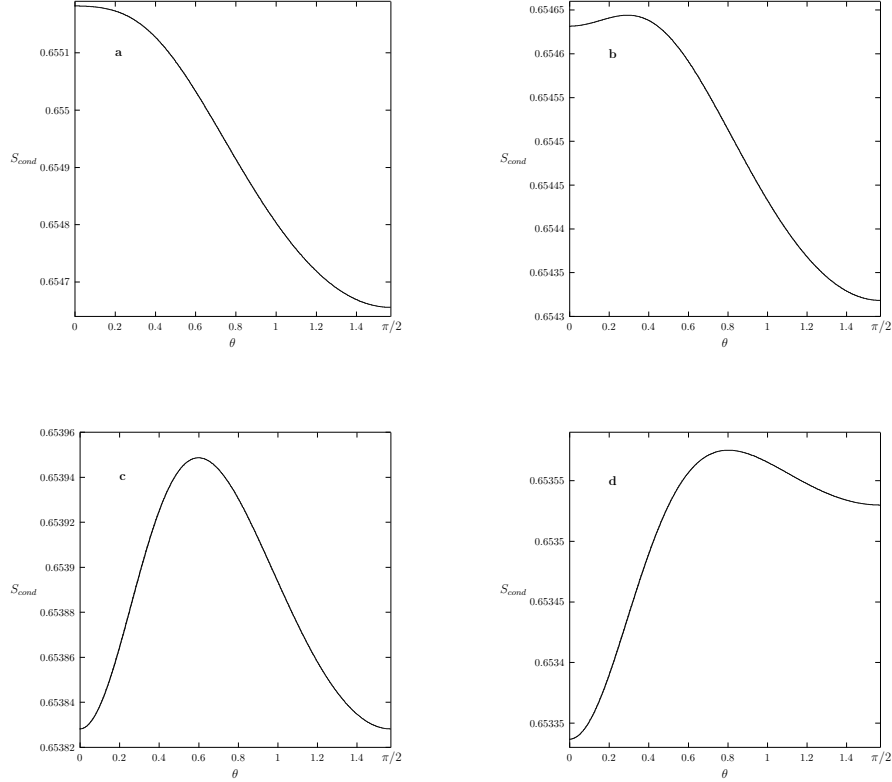


Figure 8: Conditional entropy S_{cond} (in *bits*) vs measurement angle θ by $c_3 = 0.34$, $c_1 = 0.14$, and $s_1 = 0.6477$ (a), 0.648 (b), $0.648\ 435\ 2971$ (c), and 0.6487 (d). Graphs show the evolution of intermediate maximum

of function $S_{cond}(\theta)$ can be a straight line from zero up to $\pi/2$ (type *I*). This situation is realized, for example, by $s_1 = c_1 = c_3 = 0$ or, say, by $s_1 = 0$ and $c_1 = \pm c_3$. As follows from Eq. (25), here $S_{cond}(\theta; 0, c_1, \pm c_1) = \ln 2 \text{ nat}$ ($=1$ bit) for $\forall \theta \in [0, \pi/2]$. Secondly, there are monotonically increasing or, v.v, decreasing behaviors in the whole closed interval $[0, \pi/2]$ (types *II* and *III*, respectively). Such shapes of conditional entropy lead to the Q_0 and $Q_{\pi/2}$ fractions, respectively. In the both cases, there is only one inflection point inside the interval $(0, \pi/2)$. Thirdly, the conditional entropy can has a local minimum inside the interval $(0, \pi/2)$. This is the *IV* type of its behavior. In such a case, the intermediate phase of quantum discord Q_{θ^*} arises. And finally, we have found regions in the space of X states where the conditional entropy exhibits a local maximum in the interior of interval $(0, \pi/2)$. This is the *V* type of conditional entropy behavior.

Both the minimum and maximum suddenly appear and disappear at the end points of interval $[0, \pi/2]$ through a bifurcation mechanism. Boundaries for such regions satisfy the same equations (2). To distinguish the types of regimes (*IV* or *V* according to the presented above classification) it is needed to perform an additional analysis, namely it is required to study the shapes of conditional entropy between the found boundaries.

The region with conditional entropy minimum (the θ -phase of discord) is very tiny and possibilities are not seen to observe it experimentally. On the other hand, the region with conditional entropy maximum is remarkably larger and there exists a hope to obtain the

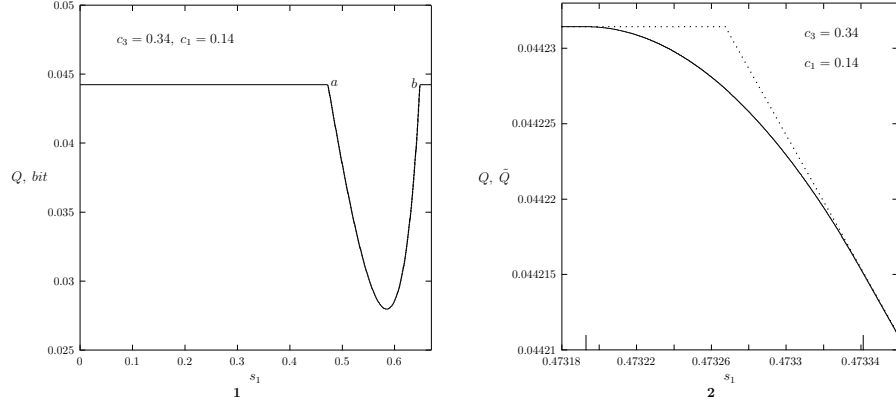


Figure 9: On **1**, it is shown the quantum discord Q vs s_1 along the straight line $c_1 = 0.14$ in the plane $c_3 = 0.34$. On **2**, it is shown the true discord Q (solid line) and false discord \tilde{Q} (dotted line) near the point a . Longer bars marks the bounds $s_1^0 = 0.4731928814$ and $s_1^{\pi/2} = 0.4733412570$ between which the Q_{θ^*} fracture exists

experimental evidence for its presence.

The branches Q_0 , $Q_{\pi/2}$, and Q_{θ^*} are analytic dependencies but the quantum discord at boundaries between them experience the sudden changes which can be observed in their higher derivatives.

As a whole one should say the following. Evaluation of quantum discord for X states with nonzero local Bloch vectors is far from completeness and perfection of Luo's formula. Above all, the unimodality of conditional entropy stays an open question. Discussion of this problem is given in the Appendix. Further, we do not know where the regions with inner minimum and maximum are located in the full five-parameter X space and which are their characteristics: values of extrema, sizes of such regions, etc. One can hope that the answers to these and other questions will be found from the future investigations.

Acknowledgment The research was supported by the RFBR Grant 15-07-07928.

Appendix. Unimodality hypothesis for X states

Here, we formulate the unimodality hypothesis for the conditional entropy and post-measurement entropy (entropy after measurements) of two-qubit X states. These entropies enter in the expressions of quantum discord and one-way quantum deficit, respectively. Start with definitions and enumerate some known facts in this mathematical field.

Definition of strong unimodality. A function $f(x)$ is a unimodal function in the interval $[a, b]$ if for some value $x_m \in [a, b]$, it is monotonically increasing for $x \leq x_m$ and monotonically decreasing for $x \geq x_m$. In that case, the maximum value of $f(x)$ is $f(x_m)$ and there are no other local maxima.

Definition of weak unimodality. A function $f(x)$ is a weakly unimodal function in the interval $[a, b]$ if there exists a value $x_m \in [a, b]$ for which it is weakly monotonically increasing for $x \leq x_m$ and weakly monotonically decreasing for $x \geq x_m$. In that case, the maximum value $f(x_m)$ can be reached for a continuous range of values of x .

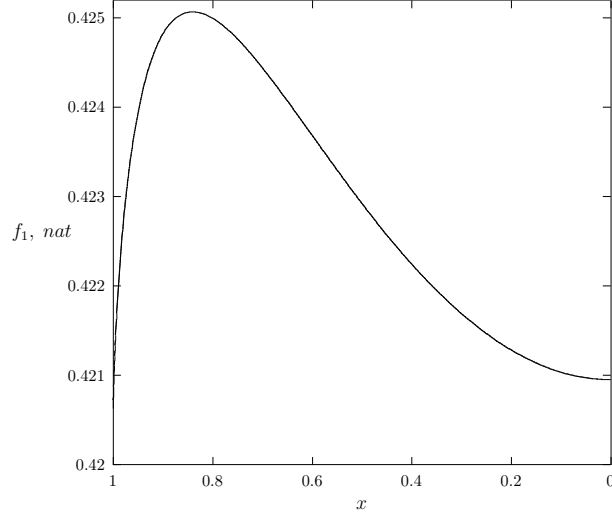


Figure 10: Behavior of function f_1 , Eq. (A1), vs x by $p_1 = p_2 = 0.25$, $p_3 = p_4 = 0.656$, and $p_5 = -0.5$

Analogous definitions are given for the minimum. Simplest examples provide the polynomial function of second degree, $f(x) = ax^2 + bx + c$.

Proving unimodality for nontrivial functions is often hard. A general method based on derivatives is discussed in Ref. [32].

Obviously, the function is unimodal one if it is convex/concave in the interval $[a, b]$. This is a sufficient condition. Further, f is unimodal if there is a one to one differentiable mapping $x = g(y)$ such that $f(g(y))$ is convex/concave. The latter allows to prove the unimodality property in some cases.

We consider two functions of one variable $x \in [0, 1]$ with five real parameters p_1, \dots, p_5 ,

$$f_1(x; p_1, p_2, p_3, p_4, p_5) = -h_2\left(\frac{1+p_2x}{2}, \frac{1-p_2x}{2}\right) + h_4\left(\frac{1+p_2x+\sqrt{r_1}}{4}, \frac{1+p_2x-\sqrt{r_1}}{4}, \frac{1-p_2x+\sqrt{r_2}}{4}, \frac{1-p_2x-\sqrt{r_2}}{4}\right) \quad (\text{A1})$$

and

$$f_2(x; p_1, p_2, p_3, p_4, p_5) = h_4\left(\frac{1+p_2x+\sqrt{r_1}}{4}, \frac{1+p_2x-\sqrt{r_1}}{4}, \frac{1-p_2x+\sqrt{r_2}}{4}, \frac{1-p_2x-\sqrt{r_2}}{4}\right) \quad (\text{A2})$$

with $r_{1,2} = (p_1 \pm p_5x)^2 + 4w^2(1-x^2)$ and $w = (|p_3 + p_4| + |p_3 - p_4|)/4$. These functions, $f_1(x)$ and $f_2(x)$, correspond to the conditional entropy [20] and entropy after measurements [21, 33]⁴, respectively.

In the expressions (A1) and (A2), $h_2(x_1, x_2) = -x_1 \log x_1 - x_2 \log x_2$ with additional condition $x_1 + x_2 = 1$ and $h_4(x_1, x_2, x_3, x_4) = -x_1 \log x_1 - x_2 \log x_2 - x_3 \log x_3 - x_4 \log x_4$ with condition $x_1 + x_2 + x_3 + x_4 = 1$ are, respectively, the binary and quaternary entropy

⁴ Results of papers [21, 33] are restricted to $p_3 + p_4 \geq 0$ and $p_3 - p_4 \geq 0$ (one needs every time to reduce the initial X density matrix to a form with nonnegative off-diagonal entries) whereas our expressions (A1) and (A2) are automatically valid in the whole domain \mathcal{D} thanks to the quantity w [18, 19, 20].

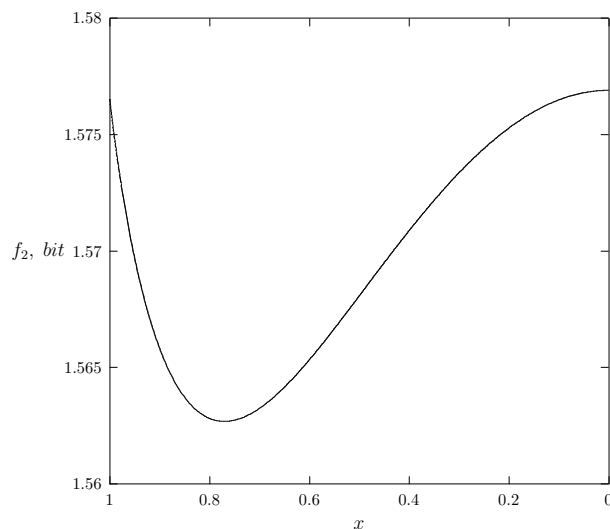


Figure 11: Behavior of function f_2 , Eq. (A2), vs x by $p_1 = p_2 = 0.385$, $p_3 = p_4 = -0.615$, and $p_5 = -0.23$

Shannon functions; $0 \leq h_2 \leq 1$ bit and $0 \leq h_4 \leq 2$ bits. These functions are convex [34, 35]. It is known also that the sum of convex functions is convex again but the difference is not in general.

Conjecture. The functions $f_1(x)$ and $f_2(x)$ for every choice of parameters p_1, \dots, p_5 for which all arguments of Shannon functions are non-negative can have at most only a one local extremum (minimum or maximum) in the open interval $x \in (0, 1)$.

It is required to prove or refute this proposition. Numerical calculations [18, 19, 20, 21] give evidences which support the above conjecture. Figures 10 and 11 show the dependencies of $f_1(x)$ and $f_2(x)$ for specific choice of parameters p_1, \dots, p_5 . Notice that the used mapping $x = \cos \theta$ has led, as seen from the figures, to convexity/concavity of both functions for $x \geq x_m$ unlike the same quantities upon the angle θ . So, it is enough to find an additional mapping which provides convexity/concavity below the extremal points x_m .

References

- [1] Modi, K., Brodutch, A., Cable, H., Paterek, T., Vedral, V.: The classical-quantum boundary for correlations: discord and related measures. *Rev. Mod. Phys.* **84**, 1655 (2012)
- [2] Streltsov, A.: Quantum correlations beyond entanglement and their role in quantum information theory. SpringerBriefs in Physics. Springer, Berlin (2015); arXiv:1411.3208v1 [quant-ph]
- [3] Adesso, G., Bromiey, T.R., Cianciaruso, M.: Measures and applications of quantum correlations. *J. Phys. A: Math. Theor.* **49**, 473001 (2016)

- [4] Brodutch, A., Terno, D.R.: Why should we care about quantum discord? in: Lectures on general quantum correlations and their applications, ed. Fanchini, F.F., Soares-Pinto, D.O., Adesso, G.; arXiv:1608.01920v1 [quant-ph]
- [5] Zurek, W.H.: Einselection and decoherence from an information theory perspective. *Ann. Phys. (Leipzig)* **9**, 855 (2000)
- [6] Ollivier, H., Zurek, W.H.: Quantum discord: a measure of the quantumness of correlations. *Phys. Rev. Lett.* **88**, 017901 (2001)
- [7] Zurek, W.H.: Quantum discord and Maxwell's demons. *Phys. Rev. A* **67**, 012320 (2003)
- [8] Luo, S.: Quantum discord for two-qubit systems. *Phys. Rev. A* **77**, 042303 (2008)
- [9] Ali, M., Rau, A.R.P., Alber, G.: Quantum discord for two-qubit X states. *Phys. Rev. A* **81**, 042105 (2010); Erratum in: *Phys. Rev. A* **82**, 069902(E) (2010)
- [10] Lu, X.-M., Ma, J., Xi, Z., Wang, X.: Optimal measurements to access classical correlations of two-qubit states. *Phys. Rev. A* **83**, 012327 (2011)
- [11] Chen, Q., Zhang, C., Yu, S., Yi, X.X., Oh, C.H.: Quantum discord of two-qubit X states. *Phys. Rev. A* **84**, 042313 (2011)
- [12] Lu, X.-M., Xi, Z., Sun, Z., Wang, X.: Geometric measure of quantum discord under decoherence. *Quantum Inf. Comput.* **10**, 0994 (2010)
- [13] Ciliberti, L., Rossignoli, R., Canosa, N.: Quantum discord in finite XY chains. *Phys. Rev. A* **82**, 042316 (2010)
- [14] Vinjanampathy, S., Rau, A.R.P.: Quantum discord for qubit-qudit systems. *J. Phys. A: Math. Theor.* **45**, 095303 (2012)
- [15] Huang, Y.: Quantum discord for two-qubit X states: analytical formula with very small worst-case error. *Phys. Rev. A* **88**, 014302 (2013)
- [16] Maldonado-Trapp, A., Hu, A., Roa, L.: Analytical solutions and criteria for the quantum discord of two-qubit X -states. *Quantum Inf. Process.* **14**, 1947 (2015)
- [17] Jing, N., Yu, B.: Quantum discord of X -states as optimization of a one variable function. *J. Phys. A: Math. Theor.* **49**, 385302 (2016)
- [18] Yurischev, M.A.: Quantum discord for general X and CS states: a piecewise-analytical-numerical formula. arXiv:1404.5735v1 [quant-ph]
- [19] Yurishchev, M.A.: NMR dynamics of quantum discord for spin-carrying gas molecules in a closed nanopore. *J. Exp. Theor. Phys.* **119**, 828 (2014); arXiv:1503.03316v1 [quant-ph]
- [20] Yurischev, M.A.: On the quantum discord of general X states. *Quantum Inf. Process.* **14**, 3399 (2015)
- [21] Ye, B.-L., Wang, Y.-K., Fei, S.-M.: One-way quantum deficit and decoherence for two-qubit X -states. *Int. J. Theor. Phys.* **55**, 2237 (2016)

- [22] Arnold, V.I.: Catastrophe theory. Springer, Berlin (1992), sec. 10
- [23] Kim H., Hwang M.-R., Jung E., Park D.K.: Difficulties in analytic computation for relative entropy of entanglement. *Phys. Rev. A* **81**, 052325 (2010)
- [24] Nguyen, N.T.T., Joynt, R.: Topology of quantum discord. arXiv:1310.5286v1 [quant-ph]
- [25] Horodecki R., Horodecki M.: Information-theoretic aspects of inseparability of mixed states. *Phys. Rev. A* **54**, 1838 (1996)
- [26] Moreva, E., Gramegna, M., Yurischev, M.A.: Exploring quantum correlations from discord to entanglement. *Adv. Sci. Eng. Med.* **9**, 46 (2017); arXiv:1612.04589v1 [quant-ph]
- [27] Céleri, L.C, Maziero, J.: The sudden change phenomena of quantum discord. in: Lectures on general quantum correlations an their applications, ed. Fanchini, F.F., Soares-Pinto, D.O., Adesso, G.; arXiv:1610.02882v1 [quant-ph]
- [28] Klobus, W., Grudka, A., Baumgartner, A., Tomaszewski, D., Schönenberger, C., Martinek, J.: Entanglement witnessing and quantum cryptography with nonideal ferromagnetic detectors. *Phys. Rev. B* **89**, 125404 (2014)
- [29] Rožek, P., Busz, P., Klobus, W., Tomaszewski, D., Grudka, A., Baumgartner, A., Schönenberger, C., Martinek, J.: Entanglement detection with non-ideal ferromagnetic detectors. *Acta Phys. Pol. A* **127**, 493 (2015)
- [30] Majd, N., Ghasemi, Z.: Lower limits of spin detection efficiency for two-parameter two-qubit (TPTQ) states with non-ideal ferromagnetic detectors. *Quantum Inf. Process.* **15**, 4137 (2016)
- [31] Jiang, F.-J., Ye, J.-F., Yan, X.-H., Lü, H.-J.: Characterizing the dynamics of quantum discord under phase damping with POVM measurements. *Chin. Phys. B* **24**, 100304 (2015)
- [32] Barthelemy, T.: On the unimodality of METRIC Approximation subject to normally distributed demands. , (2013); Wikipedia, the paper “Unimodality”
- [33] Ye, B.-L., Fei, S.-M.: A note on one-way quantum deficit and quantum discord. *Quantum Inf. Process.* **15**, 279 (2016)
- [34] Cover, T.I., Thomas, J.A.: Elements of information theory. Wiley, New York (1991)
- [35] Kudryashov, B.D.: Teoriya informatsii. (2009)[in Russian]